processes

MDPI

Review

Pulsed Current Cathodic Protection for Oil and Gas Pipelines: Current Status, Challenges, and Future Trends

Kai Jin [1], Chao Yang [1,*] and Bingfan Li [2]

[1] Technology Inspection Center of Shengli Oilfield, SINOPEC, Dongying 257000, China
[2] School of Vehicle and Energy, Yanshan University, Qinhuangdao 066004, China; libingfan@ysu.edu.cn
* Correspondence: yangchao201001@163.com

Abstract

Oil and gas pipelines are critical energy infrastructure, and their external corrosion protection affects public safety and economic operation. Pulsed current cathodic protection (PCCP) replaces continuous direct current with a periodically modulated output. This critical narrative review examines its mechanisms, operating parameters, applications, and engineering limitations. The evidence includes laboratory experiments, numerical models, and a limited number of field reports. Some studies report improved potential distribution or lower current demand, but these findings depend on the waveform, soil or electrolyte, coating condition, and comparison criterion. Double-layer charging contributes to the transient response; it does not independently establish sustained off-period protection, energy savings, or an increased protection distance. Pulse-related hydrogen evolution and coating damage also require separate assessment. Particular challenges include heterogeneous and frozen soils, stray-current interference, and interpretation of time-dependent protection potentials. Priorities are matched pulse–DC comparisons, independently validated models, synchronized monitoring, and long-term field measurements. The review identifies the evidence needed to evaluate PCCP for oil and gas pipelines without assuming that results from one installation are transferable to another.

Keywords: cathodic protection; pipeline protection; pulsed current; oil and gas pipelines

1. Introduction

Globally, pipeline transportation has become a primary means of conveying oil and natural gas, owing to its low transportation cost and continuity [1,2]. However, buried steel pipelines are subject to corrosion degradation during long-term service in complex soil environments. Wall thinning, perforation leakage, and fracture failure can cause economic losses and threaten public safety. External corrosion arises from electrochemical reactions between the metal and the surrounding electrolyte. When the pipeline surface contacts soil moisture or groundwater, local differences in the metal and electrolyte establish anodic and cathodic regions. Iron dissolves at anodic sites, while cathodic reactions such as oxygen reduction sustain the electrochemical process.

The dual-protection strategy of an anticorrosion coating combined with cathodic protection (CP) is widely used for buried steel pipelines [3,4]. The coating physically isolates the metal from the corrosive medium. CP supplies cathodic current to reduce anodic dissolution at exposed steel. Cathodic protection technologies are commonly classified as sacrificial anode cathodic protection (SACP) and impressed current cathodic protection (ICCP) [5,6]. SACP uses less noble metals, such as magnesium, zinc, or aluminum, as

Check for updates

Academic Editor: Youguo Yan

Received: 20 September 2026
Revised: 27 October 2026
Accepted: 31 October 2026
Published: 2 November 2026

Copyright: © 2026 by the authors. Licensee MDPI, Basel, Switzerland. This article is an open access article distributed under the terms and conditions of the Creative Commons Attribution (CC BY) license.

consumable anodes. It requires no external power supply, but its driving voltage and current output limit its application in some high-resistivity environments. ICCP uses an external power supply and auxiliary anodes, allowing adjustment of voltage and current. Its performance nevertheless depends on soil resistance, coating condition, and anode configuration [4].

With continuous direct current (DC), an unsuitable design or changing environment can produce excessive polarization near a drain point and insufficient polarization at remote defects. Coating shielding can further restrict current access [3,7–10]. These problems motivate waveform control but do not establish an inherent deficiency of every DC installation or universal superiority of pulsing.

PCCP employs a periodically modulated cathodic output, described by pulse amplitude, frequency, pulse width, duty cycle, and waveform [11]. During a pulse, current is divided between interfacial charging and Faradaic reactions; during the off-period, the interfacial potential relaxes. Residual polarization depends on reaction kinetics, transport, coating geometry, and electrical resistance [4,12]. Laboratory studies and field reports have investigated coating-disbondment protection, potential distribution, and current demand [13–18]. Their different conditions require separate assessment of protection distance, energy consumption, hydrogen evolution, and coating integrity.

This critical narrative review examines the mechanisms, characteristic parameters, applications, and challenges of PCCP for oil and gas pipelines. Zhao et al. [11] previously reviewed mechanisms, parameters, challenges, and development trends. The present review emphasizes charge-balance constraints, evidence classification, parameter transferability, and the distinction between waveform measurement and demonstrated corrosion control. Direct pulsed-protection studies are distinguished from DC, alternating-current (AC), and structural background research. The literature was supplemented through targeted searches for pulse protection, disbonded coatings, soil resistance, waveform optimization, and monitoring, with bibliographic checks against publisher and DOI records. This is a selective critical synthesis rather than an exhaustive systematic review or bibliometric analysis; no reproducible field-wide publication census or PRISMA screening dataset is claimed.

2. Mechanism of Pulsed Current Cathodic Protection Technology

2.1. Traditional Cathodic Protection

Corrosion of oil and gas pipelines in soil environments is an electrochemical process. Anodic iron dissolution is coupled to cathodic reactions. In neutral or alkaline aqueous media, the oxygen reduction reaction (ORR) and hydrogen evolution reaction (HER) are represented by Equations (1) and (2), respectively [19].

$$O_2 + 2H_2O + 4e^- \rightarrow 4OH^- \quad (1)$$

$$2H_2O + 2e^- \rightarrow H_2 + 2OH^- \quad (2)$$

Both reactions generate hydroxide, while Equation (1) consumes oxygen and Equation (2) generates hydrogen under sufficiently negative polarization [20]. Martinelli-Orlando et al. [19] combined electrochemical measurements with in situ and ex situ characterization under sustained potentiostatic DC polarization. They linked interfacial alkalization and oxygen depletion to changes in reaction kinetics and, depending on polarization conditions, formation of an iron oxide film (Figure 1). These findings explain why protection is not determined by potential alone. They do not demonstrate persistence of the same pH profile or Fe_3O_4 film during a PCCP cycle. Pulse-resolved measurements are needed to establish how interrupted polarization changes film formation, dissolution, and hydrogen evolution.

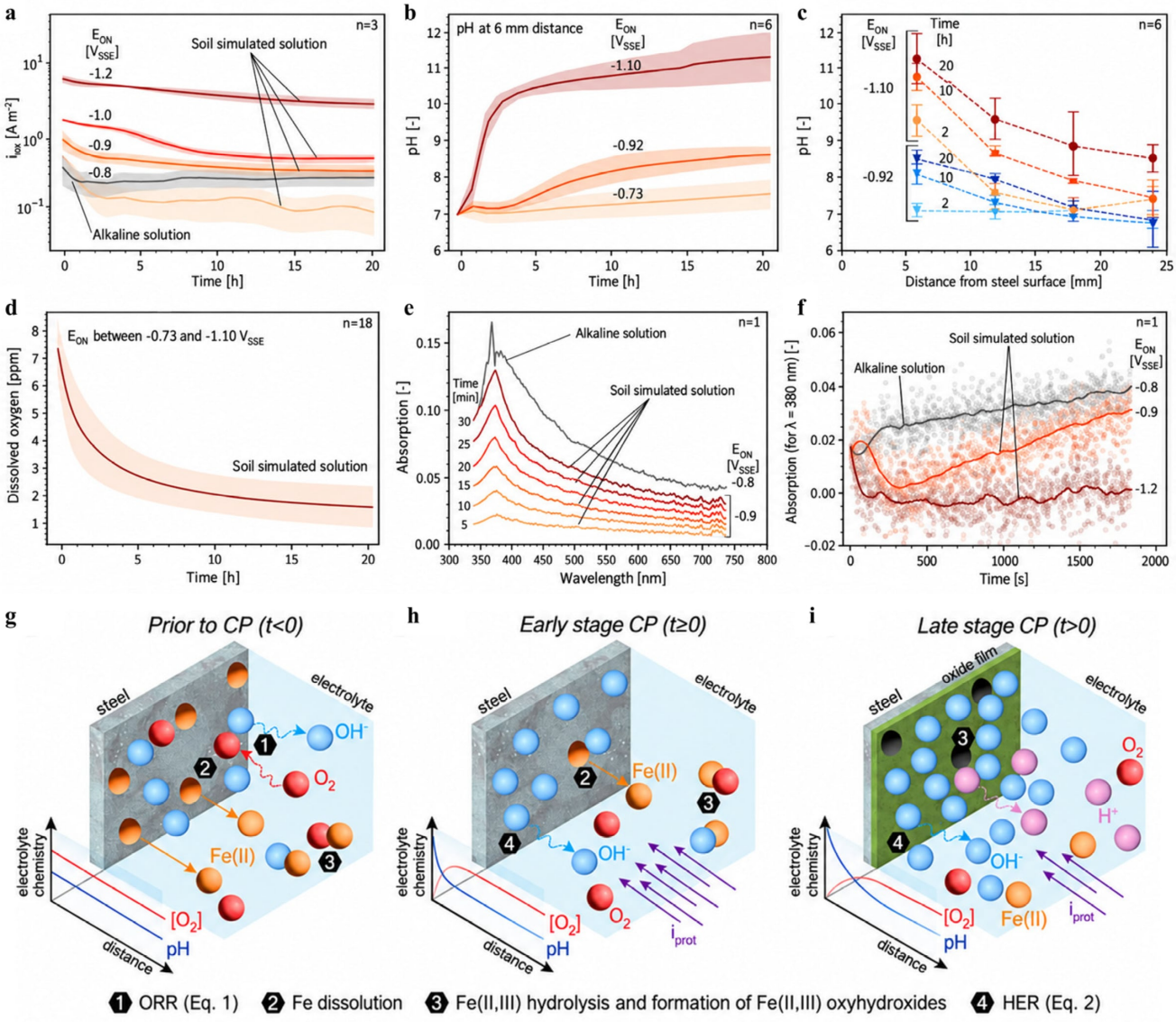

Figure 1. Interfacial changes under sustained potentiostatic DC cathodic protection. Reproduced from Martinelli-Orlando et al. [19] under the Creative Commons Attribution 4.0 International license (CC BY 4.0). (**a**) Applied protection-current response; (**b**) pH evolution 6 mm from the steel surface; (**c**) pH profiles with distance and time; (**d**) dissolved-oxygen evolution; (**e**) optical absorption spectra; (**f**) absorbance at 380 nm; (**g**–**i**) reaction and transport schematics before, during early, and during later polarization. ORR and HER are defined in Equations (1) and (2). The applied protection current and potential should not be interpreted as the free-corrosion current and potential.

Traditional cathodic protection uses SACP or ICCP (Figure 2a,b). SACP supplies current through preferential dissolution of a less noble anode, whereas ICCP supplies current from an external power source. Protection requires assessment of the steel-to-electrolyte potential, coating condition, and environmental chemistry [3,6,21,22]. A single unqualified pipe-to-soil potential does not establish protection in every soil or under interference. The on-land pipeline framework is provided by ISO 15589-1:2026 [23]; reference electrode, ohmic-drop treatment, and operating conditions must be specified when comparing protection potentials.

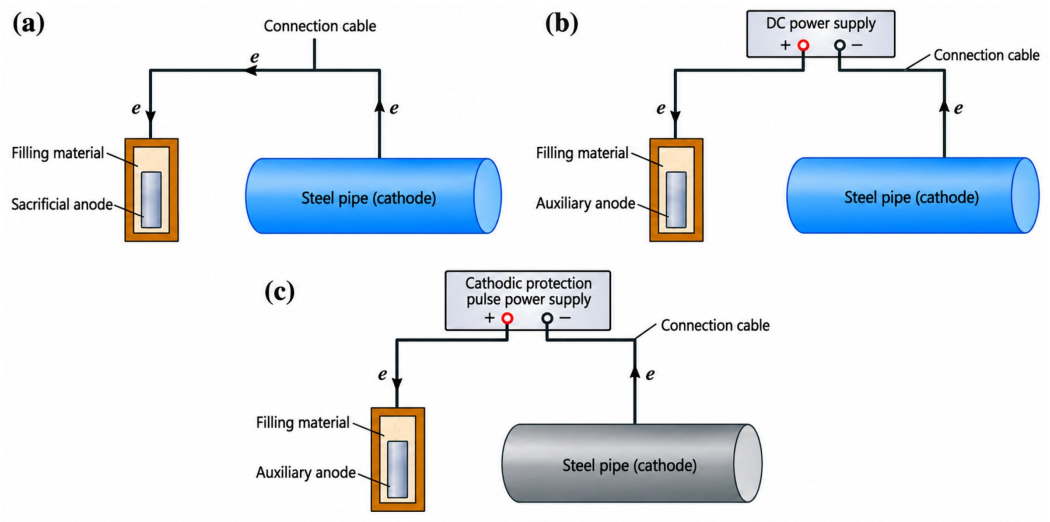

Figure 2. Redrawn schematic configurations of (**a**) sacrificial anode cathodic protection, (**b**) impressed current cathodic protection, and (**c**) pulsed-current cathodic protection.

2.2. Pulsed Current Cathodic Protection

PCCP employs discontinuous, periodically modulated current instead of continuous DC. Dedicated switching power supplies can generate different waveform shapes (Figure 3) [24]. For an ideal rectangular pulse with zero off-current, frequency equals the inverse period, duty cycle equals on-time divided by period, and mean current equals duty cycle multiplied by peak current. Frequency, pulse width, and duty cycle are therefore linked rather than independently adjustable. A lower mean applied current alone does not establish equal corrosion protection or lower total energy consumption.

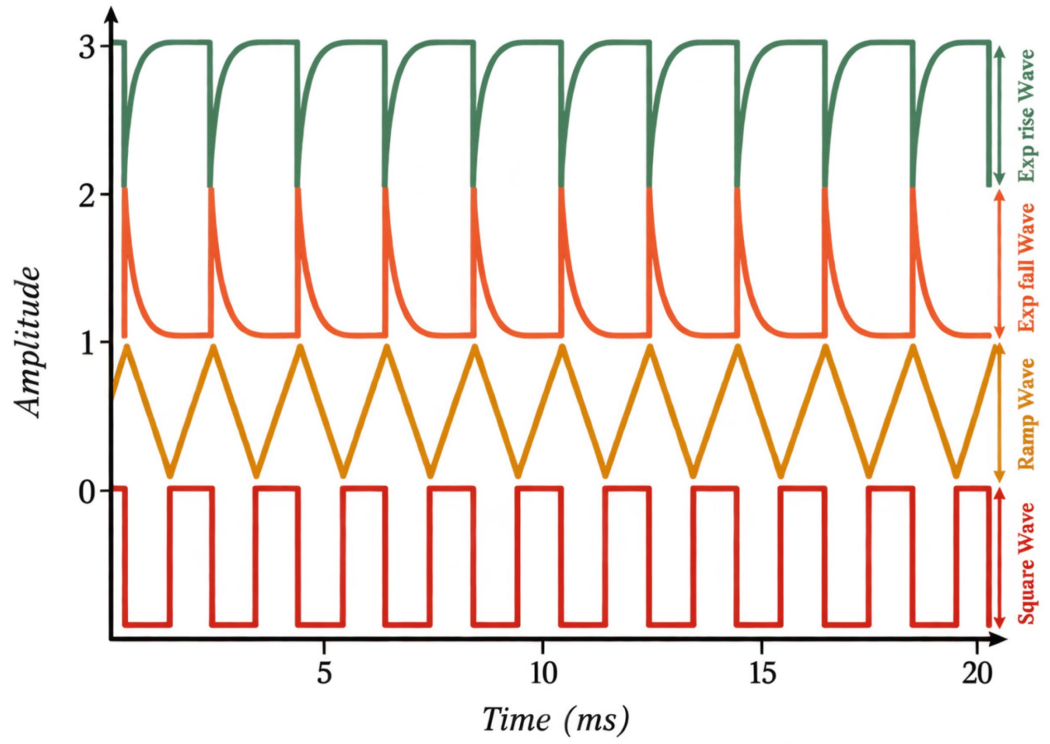

Figure 3. Illustrative waveform shapes in arbitrary units, including square, ramp, exponential-rise, and exponential-fall forms. Polarity, offset, and amplitude must be specified for a cathodic-protection application; these schematic curves are not protection criteria. Source: Eslamian et al. [25].

A minimal local equivalent circuit places the double-layer capacitance in parallel with a Faradaic branch and includes the solution or soil resistance in series. A charge-transfer resistance is a local linearization of the Faradaic branch; coating defects, concentration gradients, and pipeline geometry can require distributed elements [4,12,26]. Qiu et al. [12,27] observed resistance–capacitance (RC) responses on Q235 steel in NaCl solutions and tap water, with an important solution-resistance contribution to the measured waveform.

Capacitive sufficiency must be tested by comparing stored charge with the Faradaic charge consumed during the off-period. For approximately constant differential capacitance per unit area, the available capacitive charge is the capacitance multiplied by the allowable interfacial potential change. The required off-period charge is the time integral of the magnitude of the net Faradaic current density. Sustained protection by capacitive discharge requires that the former be sufficient for the latter while the interfacial potential remains acceptable. The cited systems do not provide a common set of capacitance, allowable potential excursion, and time-resolved Faradaic current values from which a universal sufficiency calculation can be made.

$$q_{cap} \approx C_{dl}|\Delta E| \tag{3}$$

$$q_{F,off} = \int_{off} |j_F(t)|\, dt \tag{4}$$

where q_{cap} and $q_{F,off}$ are the charges per unit area, C_{dl} is the differential capacitance per unit area, ΔE is the allowed interfacial potential excursion, and j_F is the net Faradaic current density. Equations (3) and (4) are charge-accounting relations, not a validated equivalent-potential criterion.

At periodic steady state, capacitive charge is replenished each cycle, and its net change over a complete period is zero. Capacitance redistributes current in time; it supplies no net charge source. Power comparisons require integration of the measured voltage–current product over a cycle and inclusion of converter losses. Neither lower duty cycle nor an RC response proves energy savings, prolonged off-period protection, or an increased protection distance [28].

Pulse parameters influence both polarization and transport, but reported preferences are system-specific. Wardan et al. [29] tested low-carbon steel for 14 days in 3.5 wt% NaCl using 4, 20, 50, and 100 Hz in a zero-charge corrosion-protection system. The lowest corrosion within that matrix occurred at 50 Hz. This does not establish a buried-pipeline optimum or demonstrate electron enrichment in the steel surface. A skin-effect attribution requires an appropriate electromagnetic model and independent evidence, rather than inference from corrosion rate alone.

Xu and Zhou [30] investigated frequency, duty cycle, and anode distance in an oil-well-casing system. Afshari et al. [16] compared 50 and 60 kHz at 50% and 73% duty cycle in a city gas station, reporting the most uniform potential within that matrix at 50 kHz and 73%. Eslamian et al. [31] studied API 5L X65 steel over 2–10 kHz and 25–75% duty cycle. Their preferred 10 kHz and 50% combination is likewise conditional. These distinct results do not define a universal frequency or duty cycle.

Coating disbondment creates a restricted electrolyte path that can shield steel from CP [32,33]. Najafi et al. [14] compared DC and pulse protection applied at −870 mV versus a saturated calomel electrode (SCE) at the mouth of a 20 cm simulated disbondment on X52 steel. Frequencies of 1, 5, and 10 kHz produced different potential and pH distributions, with improved corrosion mitigation at the higher tested frequencies. Wu et al. [34] examined X80 steel beneath a 250 mm simulated disbondment in soil-simulating solution. Local polarization improved under some pulse conditions, yet the potential became less negative with increasing crevice depth. Pulsing therefore did not eliminate geometric shielding.

Current access and coating preservation are separate outcomes [35]. Eslamian et al. [36] found increased cathodic-current permeability and water uptake in fusion-bonded epoxy (FBE) under pulsed operation, together with greater coating alteration. Wang et al. [13] directly examined pulse-related epoxy disbondment, while conventional-CP ageing experiments show that greater current permeability need not generate sufficient alkalization [37]. Calcareous-deposit studies in artificial seawater [38,39] concern a different electrolyte and film chemistry and cannot establish soil-pipeline performance.

A PCCP installation comprises a controllable power supply, auxiliary anodes, reference electrodes, the protected structure, and data acquisition. High peak current can intensify HER during the on-period. Experiments linking HER to epoxy delamination [40] and potential-dependent hydrogen permeation in X65 steel [41] show why reduced mean current cannot be used as a proxy for reduced hydrogen damage [42–44]. Hydrogen generation or uptake and coating disbondment should be measured alongside corrosion and electrical power under matched pulse–DC conditions. Table 1 summarizes the comparison between continuous DC and pulsed cathodic protection and the conditions for interpreting their performance.

Table 1. Comparison of continuous DC and pulsed cathodic protection with conditions for interpretation.

Comparison	Continuous DC Protection	Pulsed Protection and Interpretation	Evidence
Applied current	Continuous output, adjustable within system limits	Periodically modulated output; frequency, width, and duty cycle are linked	[11,12]
Interfacial response	Faradaic reactions and evolving chemistry/films	Charging and Faradaic reactions coexist; soil resistance and relaxation must be included	[4,12,19]
Current and energy	Demand depends on corrosion target, geometry, and environment	Lower mean current is not equivalent to lower total energy at equal protection	[28,31]
Potential distribution and distance	Dependent on soil, coating, and anode geometry	Improvements are installation-specific; pulse attenuation can limit transmission	[15,16,45,46]
Disbonded coatings	Shielding depends on access geometry and transport	Some crevice experiments improve polarization; deep regions can remain underprotected	[14,34]
Hydrogen and coating damage	Excessive cathodic polarization may drive HER and delamination	High pulse peaks may also drive HER; permeability and coating preservation differ	[13,36,40,41]

3. Applications and Research Status of PCCP in Oil and Gas Pipelines

3.1. Applications of PCCP in Oil and Gas Pipelines

Published applications include buried steel pipelines, well casings, and station installations [47–49]. Doniguian and Robinson [15] reported improved remote protection distribution on a 35-mile buried steel pipeline after installation of a pulse rectifier. The accessible conference abstract does not establish a quantified hydrogen benefit or a general energy-saving factor. A city-gas-station comparison provides a more recent installation-specific evaluation [16].

The well-casing literature also contains unfavorable or conditional findings [50]. Metwally et al. [45] combined field measurements with boundary-element analysis and found that approximately 3 kHz voltage pulses could produce predominantly DC current with superimposed ripple in an electrical submersible pump (ESP) casing system. Subsequent work associated pulse attenuation and protection distribution with deposits, soil resis-

tivity, stratification, and anode configuration [46,51]. Well-casing observations and models [30,52] therefore inform transmission limits but cannot be transferred directly to oil and gas pipelines.

3.2. Direct Evidence and Parameter Transferability

The evidence comprises laboratory comparisons, numerical models, and limited field reports, addressing different performance endpoints. Table 2 compares selected direct pulse-protection studies and their boundaries. It does not count structural pipe tests or AC-interference simulations as PCCP efficacy studies. A comparison needs the material, electrolyte or soil resistance, coating geometry, waveform, reference electrode, exposure time, and DC control; an optimum without these conditions is not a transferable design rule.

Doniguian, Kipps, and Barnes [53] reported the pulse cathodic protection of prestressed concrete cylinder pipe. Although the pipe type has the same abbreviation as pulsed current cathodic protection, the study is relevant to the latter technology and is retained as cross-application evidence. Its conference record does not justify the original description as a verified patent-based hardware study, nor does concrete-pipe experience establish the external protection of oil and gas steel pipelines.

By contrast, structural studies of prestressed concrete cylinder pipe [54,55] examine bearing capacity, wire corrosion, and wire breakage in prestressed concrete cylinder pipe. They provide only structural context and are excluded from Table 2 and from conclusions about pulse-protection effectiveness.

Hu et al. [55] combined full-scale testing with a structural model to examine the load-carrying effects of broken prestressing wires. Agreement between their strain measurements and mechanical simulations validates that structural model, not a PCCP corrosion-control model. The distinction avoids overstating the maturity of pulse-protection validation.

Waveform shape adds a further comparison variable. Hashemi [56] experimentally compared square, exponential, and ramp waveforms and used adaptive neuro-fuzzy inference system (ANFIS) modeling; the publisher abstract reports an optimized ramp frequency near 4.8 kHz within that study. Its skin-effect interpretation is an author attribution rather than proof of the low-frequency electron-enrichment explanation. Eslamian et al. [25] numerically compared waveform-dependent oxygen, pH, potential, and current distributions beneath a disbonded coating. Their ramp-waveform prediction is conditional on the model boundaries and is not independent field validation.

Ali et al. [57] linked waveform optimization to controlled soil burial and full-scale burst testing, extending assessment beyond potential distribution. Longer-term and independently replicated field comparisons remain necessary.

The reported 50 Hz, kilohertz, and station-scale settings are therefore not interchangeable (Table 2). A potential-distribution improvement, reduced pitting, lower coating-disbondment area, lower electrical energy, and reduced hydrogen uptake are distinct outcomes. Favorable results for one cannot establish the others. FBE studies in particular identify a trade-off between improved current access and coating alteration [13,36].

Model development should separate calibration from validation and test predictions under untrained soil, geometry, and waveform conditions. Soil and disbondment experiments [58–60] show that moisture and gap geometry are important transfer variables. A model optimized for one installation requires independent tests before its settings can be recommended for another.

Table 2. Selected pulse-protection studies and the boundaries of their parameter findings.

Study and Evidence	Material and Environment	Waveform or Tested Settings	Endpoint and Boundary
Qiu et al. [12,27] Aqueous experiment	Q235; 3% NaCl, 0.06% NaCl, tap water	Square-wave current; varying amplitude, frequency, duty cycle	Potential waveforms; resistance compensation needed. Aqueous estimator, not a soil criterion.
Doniguian and Robinson [15] Field conference report	35-mile buried steel pipeline	Pulse rectifier; detailed settings not established from accessible abstract	Remote potential distribution; no general energy or hydrogen factor derived.
Doniguian et al. [53] Cross-application report	Prestressed concrete cylinder pipe	Pulse CP; parameter extraction not supported by available record	Relevant pulse application, but different host material; not a patent-verification source.
Xu and Zhou [30] Casing model and experiments	Oil-well-casing/formation system	Square-wave pulses; frequency, duty cycle, anode distance varied	Potential distribution; geometry and formation limit transferability.
Wardan et al. [29] Laboratory conference paper	Low-carbon steel; 3.5 wt% NaCl; 14 days	4, 20, 50, 100 Hz; zero-charge protection system	Weight loss and morphology; 50 Hz preferred only within this matrix.
Najafi et al. [14] Laboratory DC/pulse comparison	X52; 20 cm simulated disbondment	1, 5, 10 kHz; −870 mV vs. SCE at crevice mouth	Potential, corrosion, pH; no universal crevice penetration.
Wang et al. [13] Coating experiment	Epoxy-coated steel	Pulse CP; detailed protocol not reconstructed from abstract	Cathodic disbondment; coating damage is a separate endpoint.
Afshari et al. [16] Station comparison	City gas station	50/60 kHz; duty cycle 50%/73%	Potential distribution; 50 kHz/73% preferred within the tested matrix.
Eslamian et al. [31] Experiment and fitted model	API 5L X65 pipeline steel	2–10 kHz; duty cycle 25–75%	Corrosion/electrical/chemical endpoints; 10 kHz/50% conditional.
Wu et al. [34] Crevice experiment	X80; soil-simulating solution; 250 mm crevice	Frequency, duty cycle, potential and gap varied	Local polarization; deeper crevice regions can remain insufficiently polarized.
Eslamian et al. [36] FBE pulse/DC comparison	Fusion-bonded epoxy coating	DC and 5/10 kHz pulsing	Current permeability and coating alteration; improved access is not preserved barrier life.
Hashemi [56] Experiments and ANFIS model	Soil-simulating system	Square, exponential rise/fall, ramp; optimized ramp near 4.8 kHz	Potential, current, deposits, pitting; optimized within its model domain.
Eslamian et al. [25] Numerical model	Disbonded-coating crevice	Alternative waveforms, including ramp	Oxygen, pH, current and potential predictions; not independent field validation.
Ali et al. [57] Model and controlled validation	Steel pipeline segments in controlled soil burial	Data-driven waveform design	Localized damage and full-scale burst testing; limited duration and replication.
Metwally et al. [45,46,51] Field/model studies	Deep well casings; soil/deposit variation	Pulsed excitation; ~3 kHz in one field system	Pulse attenuation, ripple, current distribution; installation-dependent results.

4. Challenges in the Practical Application of Pulsed Current Cathodic Protection

Laboratory and installation-specific findings leave a gap between current evidence and long-term deployment on oil and gas pipelines. The main challenges concern changing soil conditions, external electrical interference, and the relationship between a measured waveform and sustained corrosion control.

4.1. Complexity of Soil Environments Along the Pipeline

Corrosion and CP performance depend on local soil chemistry, water availability, and electrode condition. Experiments on pipeline steels have investigated potential fluctuations, local chemistry beneath disbonded coatings, and soil-solution-dependent protection parameters [61–63]. Weld condition can further change the response beneath a disbondment [64]. These findings are environmental and material background; they do not establish that pulsing removes soil resistance or suppresses corrosion in every soil.

Frozen ground provides an extreme case of seasonal environmental variation. Freeze–thaw conditions can change soil electrical properties, drainage, and the mechanical loading of pipeline coatings. The cited permafrost studies address pipeline hazards, inspection, and monitoring [65,66]. They provide no direct pulse–DC protection comparison under freezing and thawing. Accordingly, PCCP superiority in frozen soil is not established here. Tests should compare measured soil resistivity and water state with local polarization, coating integrity, and corrosion through repeated seasonal cycles. Disbondment geometry and soil saturation must also be controlled because they affect localized corrosion independently of the applied waveform [58].

4.2. Stray Current Interference

Electrified transport and power infrastructure can create external current paths through the soil and buried pipelines (Figure 4). Railway grounding and return-current configuration affect leakage and interference [67,68]. AC transmission-line simulations [69] and metro/tram investigations [70–72] concern external interference, not evidence that a pulse waveform improves protection. High-voltage direct current (HVDC) ground-return operation, illustrated in Figure 4, and AC coupling must likewise be distinguished from the imposed PCCP waveform [73].

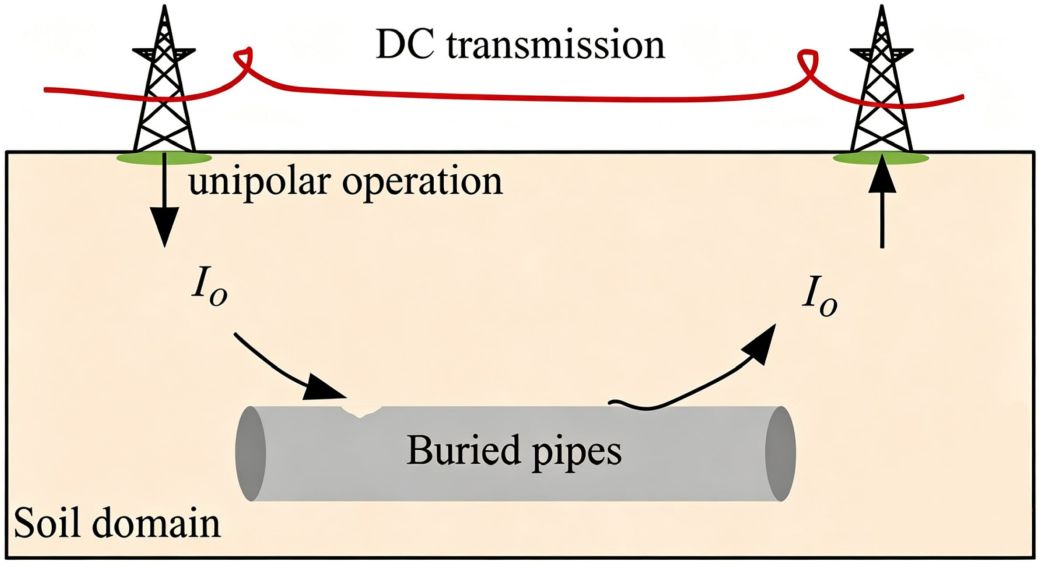

Figure 4. Schematic of external current paths associated with HVDC ground-return operation. Current entering and leaving a buried pipeline can perturb cathodic polarization. The illustration concerns external DC interference, not the imposed PCCP waveform; the HVDC interference mechanism is discussed by Chen and Li [73].

Bertolini et al. [74] studied stray-current corrosion of reinforcing steel in concrete. Because concrete alkalinity and steel condition differ from those of buried pipeline steel, their results cannot support a general claim that AC is weakly corrosive to pipelines. Peng et al. [70] instead combined a DC-tram circuit model, finite-element simulation, and pipeline-

steel electrochemical tests. Qin et al. [75] examined dynamic DC effects on X70 steel. Further tests on cathodically protected buried steel show that current magnitude and interference duration must be considered, rather than the peak potential alone [76].

Cui et al. [77] modeled and experimentally examined DC interference from CP anode groundbeds, showing dependence on pipeline and anode geometry and soil conditions. This is distinct from the X80 corrosion experiment by Xu et al. [78]. In that study, stress and AC jointly intensified corrosion; the numerical current-density increase is not used here as a PCCP benefit or penalty.

AC effects depend on CP level, medium, and material response. Pipeline-steel studies address AC-dependent stress-corrosion behavior [79–81], while a broader review discusses high-pH cracking mechanisms [82]. X70 experiments found that increasing CP current under AC did not monotonically decrease corrosion [83]. In situ and ex situ film measurements further illustrate film transformation under combined AC and high CP [84]. These are interference studies and cannot establish the response to a kilohertz cathodic pulse without direct tests.

PCCP assessments under interference should record the imposed pulse and external current histories simultaneously. Potential peaks alone cannot distinguish ohmic effects, transient depolarization, and corrosion. ISO 18086:2019 [85] addresses long-term AC interference at 16.7–60 Hz and explains why pipeline CP criteria alone are insufficient under AC [86,87]. Its scope does not validate arbitrary kilohertz pulse criteria. Combined interference and PCCP experiments remain a specific research need; DC or AC background should not be counted as pulse-protection validation.

4.3. Accuracy of Monitoring and Evaluation

Accurate evaluation of cathodic protection performance is a prerequisite for pipeline operation. Under pulsing, a measured pipe-to-soil potential includes interfacial polarization, time-dependent ohmic drop, and acquisition-system response. Current interruption may remove an ohmic component while electrochemical relaxation and switching transients continue. It is therefore too strong to claim that every instant-off value is either the true steady polarized potential or merely a capacitive artifact [28,88].

A specific proposal exists in the early pulse literature. After compensating solution resistance, Qiu et al. [12] proposed the bottommost potential of the measured cathodic waveform as an electrode-polarization estimate for their Q235 aqueous systems, where residual waveform amplitude was small. This is a study-specific estimator, not a universal soil-pipeline criterion. No validated universal sampling delay or equivalent-potential formula applicable across the systems reviewed here was established.

A defensible acquisition protocol should report the pulse-trigger reference, sampling rate, analog bandwidth and filtering, switching blanking or delay, averaging interval, reference-electrode placement, and treatment of all interruptible current sources. Candidate delayed-off, minimum, or cycle-average metrics should be compared with coupon corrosion, local chemistry, or another independent protection endpoint [89] before operational use. Selecting a delay without demonstrating separation of switching, ohmic, and polarization responses can bias the results [88]. ISO 15589-1:2026 [23] provides the on-land CP framework, but its scope statement is not evidence for a validated PCCP sampling window.

Engineering practice has nevertheless explored digital PCCP monitoring [90]. Gao et al. [91] described a system applied to two oil pipelines in the Tongzhai operating area of Changqing Oilfield in 2022. It enabled remote operating-state monitoring and adjustment with expert-system assistance. The report supports deployment feasibility, but the accessible evidence does not establish a matched energy baseline, pulse-resolved measurement accuracy, or a transferable protection-depth gain. These observations do not

establish a general energy-saving factor or protection-depth multiplier. Remote communication and control should be evaluated separately from high-speed waveform capture and corrosion protection.

5. Conclusions

- PCCP changes the temporal distribution of applied cathodic current. Double-layer charging contributes to the transient response, but a capacitance and charge balance is needed before attributing off-period protection to capacitive discharge.
- Laboratory studies and limited installation reports demonstrate conditional improvements in selected corrosion or potential-distribution endpoints. No universal optimum frequency, duty cycle, energy-saving factor, or protection-distance multiplier follows from these different systems.
- Coating permeability, coating disbondment, hydrogen uptake, corrosion rate, and electrical power are distinct outcomes. A favorable polarization result does not establish coating preservation or hydrogen safety.
- Current evidence does not establish long-term PCCP superiority in frozen soils or under combined electrical interference. Reliable deployment requires validated potential interpretation and independent corrosion measurements.

6. Future Research Priorities

- Measure capacitance, interfacial potential excursion, Faradaic current, and local chemistry together to test charge balance and film persistence during pulse cycles.
- Compare pulse and DC protection using matched materials, soils, coating defects, and protection targets. Report actual voltage/current waveforms, total energy, corrosion, coating damage, and hydrogen uptake.
- Validate waveform models beyond their calibration domain, including different soil saturation, resistivity, gap geometries, and freeze–thaw conditions. Machine-learning fit quality should be separated from independent physical validation.
- Test synchronized waveform acquisition and interference assessment against independent corrosion endpoints. Sampling windows and equivalent-potential estimators require documented validation.
- Conduct long-term field comparisons with traceable DC controls before extending laboratory findings to oil and gas pipelines. Adaptive control and alternative power supplies should follow demonstrated protection performance and contribute to evidence-based evaluation procedures.

Author Contributions: Conceptualization, K.J. and C.Y.; validation, B.L.; investigation, B.L.; writing—original draft preparation, K.J. and C.Y.; writing—review and editing, B.L. All authors have read and agreed to the published version of the manuscript.

Funding: This research received no external funding.

Data Availability Statement: No new data were created or analyzed in this study.

Conflicts of Interest: Author Kai Jin and Chao Yang were employed by the company SINOPEC (Shengli Oilfield Technology Inspection Center). The remaining author declares that the research was conducted in the absence of any commercial or financial relationships that could be construed as a potential conflict of interest. The company SINOPEC had no role in the design of the study; in the collection, analyses, or interpretation of data; in the writing of the manuscript, or in the decision to publish the results.

References

1. Bai, X.; Zhao, Y.; Xu, L. Study on Corrosion Prevention and Treatment in Long-Distance Oil and Gas Pipeline. *IOP Conf. Ser. Earth Environ. Sci.* **2019**, *384*, 012178. [CrossRef]
2. Chen, X.; Zhao, Y. Research on Corrosion Protection of Buried Steel Pipeline. *Engineering* **2017**, *09*, 504–509. [CrossRef]
3. Meroufel, A.; Gordon, A.; Thierry, D. Cathodic protection shielding of coated buried pipeline. *J. Coat. Technol. Res.* **2024**, *21*, 445–459. [CrossRef]
4. Oghli, H.M.; Akhbari, M.; Kalaki, A.; Eskandarzade, M. Design and analysis of the cathodic protection system of oil and gas pipelines, using distributed equivalent circuit model. *J. Nat. Gas Sci. Eng.* **2020**, *84*, 103701. [CrossRef]
5. Gurrappa, I.; Yashwanth, I.V.S.; Mounika, I. Cathodic Protection Technology for Protection of Naval Structures Against Corrosion. *Proc. Natl. Acad. Sci. India Sect. A Phys. Sci.* **2015**, *85*, 1–18. [CrossRef]
6. Ameh, E.S.; Ikpeseni, S.C. Pipelines cathodic protection design methodologies for impressed current and sacrificial anode systems. *Niger. J. Technol.* **2017**, *36*, 1072–1077. [CrossRef]
7. Xu, M.; Lam, C.N.C.; Wong, D.; Asselin, E. Evaluation of the cathodic disbondment resistance of pipeline coatings—A review. *Prog. Org. Coat.* **2020**, *146*, 105728. [CrossRef]
8. Chin, D.T.; Sabde, G.M. Current Distribution and Electrochemical Environment in a Cathodically Protected Crevice. *Corrosion* **1999**, *55*, 229–237. [CrossRef]
9. Perdomo, J.J.; Song, I. Chemical and electrochemical conditions on steel under disbonded coatings: The effect of applied potential, solution resistivity, crevice thickness and holiday size. *Corros. Sci.* **2000**, *42*, 1389–1415. [CrossRef]
10. Varela, F.; Tan, M.Y.J.; Forsyth, M. Understanding the effectiveness of cathodic protection under disbonded coatings. *Electrochim. Acta* **2015**, *186*, 377–390. [CrossRef]
11. Zhao, Q.; Li, H.; Luo, X.; Shi, Y.; Li, J.; Wang, C.; Liu, Y.; Lv, X. Research on Pulse Current Cathodic Protection Technology for Long-Distance Pipeline: A Review. *Mater. Corros.* **2025**, *76*, 20–28. [CrossRef]
12. Qiu, Y.; Guo, Z.; Lin, H. Mechanism of the cathodic protection by square wave pulsed currents I Characteristics of the cathodic potential waveforms. *J. Chin. Soc. Corros. Prot.* **2002**, *22*, 295–299.
13. Wang, J.; Hu, J.; Gu, C.; Mou, Y.; Yu, J.; Zhong, X. The effect of pulse current cathodic protection on cathodic disbondment of epoxy coatings. *Prog. Org. Coat.* **2022**, *170*, 107001. [CrossRef]
14. Najafi, H.; Eslami, A.; Golozar, M.A.; Kavian, A.; Ahmadi, M. Effect of pulse cathodic protection on corrosion mitigation and electrochemical conditions under a simulated coating disbondment on pipeline steel. *Mater. Corros.* **2022**, *73*, 116–124. [CrossRef]
15. Doniguian, T.M.; Robinson, R.C. Corrosion Measuring Techniques Confirm Effectiveness of Pulse Cathodic Protection for Buried Steel Pipeline. In Proceedings of the CORROSION 1999, San Antonio, TX, USA, 25–30 April 1999; pp. 1–8. [CrossRef]
16. Afshari, M.; Eslami, A.; Golozar, M.A.; Fatehi, A.; Gorji, H.R.; Ahmadi, M.; Kavian, A.; Tavosi, S.D. Investigation on utilizing pulse CP in a city gas station: A comparison with conventional CP. *J. Pipeline Sci. Eng.* **2023**, *3*, 100109. [CrossRef]
17. Brousseau, R.; Qian, S.; Gummow, B. Investigating the Effect of Pulse Cathodic Protection underneath a Disbonded Coating. *CORROSION* **1993**, *1993*, 1–8. [CrossRef]
18. Diakow, D.A.; Van Boven, G.J.; Wilmott, M.J. Polarization Beneath Disbonded Coatings: A Comparison between Conventional and Pulsed Cathodic Protection. *CORROSION* **1997**, *1997*, 1–10. [CrossRef]
19. Martinelli-Orlando, F.; Mundra, S.; Angst, U.M. Cathodic protection mechanism of iron and steel in porous media. *Commun. Mater.* **2024**, *5*, 15. [CrossRef]
20. Glass, G.K.; Chadwick, J.R. An investigation into the mechanisms of protection afforded by a cathodic current and the implications for advances in the field of cathodic protection. *Corros. Sci.* **1994**, *36*, 2193–2209. [CrossRef]
21. Refait, P.; Jeannin, M.; Fleury, E.; Raffin, F.; Fontaine, S. Cathodic Protection of Carbon Steel in Soil: A Study of Induced Passivation. *Corros. Mater. Degrad.* **2024**, *5*, 387–405. [CrossRef]
22. Mahlobo, M.G.R.; Olubambi, P.A.; Mjwana, P.; Jeannin, M.; Refait, P. Study of Overprotective-Polarization of Steel Subjected to Cathodic Protection in Unsaturated Soil. *Materials* **2021**, *14*, 4123. [CrossRef] [PubMed]
23. *ISO 15589-1:2026*; Oil and Gas Industries Including Lower Carbon Energy—Cathodic Protection of Pipeline Transportation Systems—Part 1: On-Land Pipelines. International Organization for Standardization (ISO): Geneva, Switzerland, 2026. Available online: https://www.iso.org/standard/86820.html (accessed on 30 July 2026).
24. Shurayts, A.; Maruhin, D.; Zubailov, H.; Tomashevskiy, Y. Energy efficient station for cathodic protection of underground metalic pipelines using pulsed current modes. *E3S Web Conf.* **2019**, *121*, 02010. [CrossRef]
25. Eslamian, H.; Rahimzadeh Lotfabad, F.; Hashemi, B. Finite Difference Modeling to Study Pulsed Current Cathodic Protection's Effect on Disbonded Coating Crevice Corrosion Mitigation: Waveform Effect. *J. Electrochem. Soc.* **2025**, *172*, 041501. [CrossRef]
26. Song, F.M.; Sridhar, N. A Two-Dimensional Model for Steel Corrosion Under a Disbonded Coating Due to Oxygen With or Without Cathodic Protection—Part 1: Full Numerical Solution. *CORROSION* **2006**, *62*, 676–686. [CrossRef]
27. Qiu, Y.; Guo, Z.; Lin, H. Mechanism of the cathodic protection by square wave pulsed currents II Effects of the current parameters. *J. Chin. Soc. Corros. Prot.* **2002**, *22*, 367–370.

28. Angst, U.M. A Critical Review of the Science and Engineering of Cathodic Protection of Steel in Soil and Concrete. *CORROSION* **2019**, *75*, 1420–1433. [CrossRef] [PubMed]
29. Wardan, R.; Shamsudin, S.R.; Wahid, M.F.M.; Sanusi, M.S. Effect of Pulse Frequencies on Low Carbon Steel in 3.5 wt% NaCl Solution under Zero Charge Corrosion Protection. *IOP Conf. Ser. Mater. Sci. Eng.* **2020**, *957*, 012053. [CrossRef]
30. Xu, X.Q.; Zhou, H.B. Study on the Influence of Pulse Current Cathodic Protection Parameters of Oil Well Casing. *Adv. Mater. Sci. Eng.* **2019**, *2019*, 2847345. [CrossRef]
31. Eslamian, H.; Javidi, M.; Zamani, M.R.; Dana, M.M.; Mansoori, E. Effect of pulsed current cathodic protection on pipeline steel API 5L X65 corrosion mitigation: An investigation and machine learning-assisted modeling. *Corros. Commun.* **2023**, *12*, 29–45. [CrossRef]
32. Gan, F.; Sun, Z.W.; Sabde, G.; Chin, D.T. Cathodic Protection to Mitigate External Corrosion of Underground Steel Pipe Beneath Disbonded Coating. *CORROSION* **1994**, *50*, 804–816. [CrossRef]
33. Wang, W.; Wang, Q.; Wang, C.; Yi, J. Experimental studies of crevice corrosion for buried pipeline with disbonded coatings under cathodic protection. *J. Loss Prev. Process Ind.* **2014**, *29*, 163–169. [CrossRef]
34. Wu, C.; Zhong, T.; Feng, Y.; Shi, S.; Yan, M.; Liu, W.; Gao, B. Polarization behavior of pipelines with peeled anti-corrosive coating under pulsed current cathodic protection. *Oil Gas Storage Transp.* **2024**, *43*, 649–655.
35. Mahdavi, F.; Forsyth, M.; Tan, M.Y.J. Understanding the effects of applied cathodic protection potential and environmental conditions on the rate of cathodic disbondment of coatings by means of local electrochemical measurements on a multi-electrode array. *Prog. Org. Coat.* **2017**, *103*, 83–92. [CrossRef]
36. Eslamian, H.; Keshavarz, H.; Paydar, M.H.; Hashemi, B. Permeability of Fusion-bonded epoxy coating to cathodic current: Pulsed current vs. direct current cathodic protection. *Mater. Chem. Phys.* **2024**, *319*, 129370. [CrossRef]
37. Latino, M.; Varela, F.; Tan, Y.; Forsyth, M. The effect of ageing on cathodic protection shielding by fusion bonded epoxy coatings. *Prog. Org. Coat.* **2019**, *134*, 58–65. [CrossRef]
38. Zamanzade, M.; Shahrabi, T.; Yazdian, A. Improvement of corrosion protection properties of calcareous deposits on carbon steel by pulse cathodic protection in artificial sea water. *Anti-Corros. Methods Mater.* **2007**, *54*, 74–81. [CrossRef]
39. Zamanzade, M.; Shahrabi, T.; Gharacheh, E.A. Application of Taguchi method for the characterization of calcareous deposits formed by pulse cathodic protection. *Mater. Corros.* **2007**, *58*, 710–715. [CrossRef]
40. Gu, C.; Hu, J.; Zhong, X. The coating delamination mitigation of epoxy coatings by inhibiting the hydrogen evolution reaction. *Prog. Org. Coat.* **2020**, *147*, 105774. [CrossRef]
41. Koren, E.; Hagen, C.M.H.; Wang, D.; Lu, X.; Johnsen, R. Investigating electrochemical charging conditions equivalent to hydrogen gas exposure of X65 pipeline steel. *Mater. Corros.* **2024**, *75*, 315–321. [CrossRef]
42. Cazenave, P.; Jimenez, K.; Gao, M.; Moneta, A.; Hryciuk, P. Hydrogen assisted cracking driven by cathodic protection operated at near −1200 mV CSE—An onshore natural gas pipeline failure. *J. Pipeline Sci. Eng.* **2021**, *1*, 100–121. [CrossRef]
43. Zhang, L.; Cao, W.; Lu, K.; Wang, Z.; Xing, Y.; Du, Y.; Lu, M. Effect of the cathodic current density on the sub-surface concentration of hydrogen in X80 pipeline steels under cathodic protection. *Int. J. Hydrogen Energy* **2017**, *42*, 3389–3398. [CrossRef]
44. Xing, Y.; Yang, Z.; Zhao, Q.; Qiao, L.; Yang, J.; Zhang, L. Stress-based hydrogen damage model of X80 pipeline steel and its damage risk assessment under cathodic interference. *Int. J. Press. Vessels Pip.* **2023**, *203*, 104947. [CrossRef]
45. Metwally, I.A.; Al-Mandhari, H.M.; Gastli, A.; Al-Bimani, A. Stray currents of ESP well casings. *Eng. Anal. Bound. Elem.* **2008**, *32*, 32–40. [CrossRef]
46. Metwally, I.A.; Al-Badi, A. Factors affecting pulsed-cathodic protection effectiveness for deep well casings. *Anti-Corros. Methods Mater.* **2009**, *56*, 196–205. [CrossRef]
47. Bich, N.N.; Bauman, J. Cathodic Protection of Well Casings by Pulsed Current. *CORROSION* **1994**, *1994*, 1–10. [CrossRef]
48. Bauman, J. Well Casing Cathodic Protection Utilizing Pulse Current Technology. *CORROSION* **2004**, *2004*, 1–4. [CrossRef]
49. Ma, J.; Zhang, X.; Yuan, W.; Zhou, H. Study of Cathodic Protection System for Oil Well Casings Based on Pulse Current. In Proceedings of the 2020 International Conference on Intelligent Transportation, Big Data & Smart City (ICITBS) 2020, Vientiane, Laos, 11–12 January 2020; pp. 463–467. [CrossRef]
50. Dabkowski, J. Limitations in Using Pulsed Rectifiers for Well Casing Cathodic Protection. *CORROSION* **1995**, *1995*, 1–6. [CrossRef]
51. Metwally, I.A.; Al-Badi, A.H. Analysis of different factors affecting cathodic protection for deep well casings. *Mater. Corros.* **2010**, *61*, 245–251. [CrossRef]
52. Solovyeva, V.A.; Almuhammadi, K.H.; Badeghaish, W.O. Current Downhole Corrosion Control Solutions and Trends in the Oil and Gas Industry: A Review. *Materials* **2023**, *16*, 1795. [CrossRef] [PubMed]
53. Doniguian, T.; Kipps, H.; Barnes, J. Extending the life of prestressed concrete cylinder pipe with pulse cathodic protection. In Proceedings of the Pipelines in the Constructed Environment, San Diego, CA, USA, 23–27 August 1998; pp. 367–376. Available online: https://trid.trb.org/View/498683 (accessed on 30 July 2026).
54. Zhao, P.; Si, Z.; Huang, L.; Li, Y. Effects of prestressing wire corrosion on the load response law and bearing capacity of PCCP. *Compos. Struct.* **2024**, *332*, 117933. [CrossRef]

55. Hu, B.; Fang, H.; Wang, F.; Zhai, K. Full-scale test and numerical simulation study on load-carrying capacity of prestressed concrete cylinder pipe (PCCP) with broken wires under internal water pressure. *Eng. Fail. Anal.* **2019**, *104*, 513–530. [CrossRef]
56. Hashemi, B. Mechanistic Insights Regarding the Role of Skin Effect in Pulsed Current Cathodic Protection: Experimental Studies, ML Modeling, and Multi-objective Optimization. *J. Mater. Eng. Perform.* **2026**, *35*, 16052–16077. [CrossRef]
57. Ali, I.H.; Saeidlou, S.; Singh, P.K.; Alamry, A.; Kenany, A.A.; Javidparvar, A.A. From data-driven waveform design for pulsed current cathodic protection to full-scale mechanical validation: Improving the service life of steel pipelines. *J. Pipeline Sci. Eng.* **2025**, 100428. [CrossRef]
58. Wang, K.; Varela, F.B.; Tan, M.Y. Probing dynamic and localised corrosion processes on buried steel under coating disbondments of various geometries. *Corros. Sci.* **2019**, *150*, 151–160. [CrossRef]
59. Tan, M.Y.; Bob Varela, F.; Huo, Y. An overview of recent progresses in probing and understanding corrosion under disbonded coatings. *Corros. Eng. Sci. Technol.* **2023**, *58*, 323–332. [CrossRef]
60. Perdomo, J.J.; Chabica, M.E.; Song, I. Chemical and electrochemical conditions on steel under disbonded coatings: The effect of previously corroded surfaces and wet and dry cycles. *Corros. Sci.* **2001**, *43*, 515–532. [CrossRef]
61. Dai, M.; Liu, J.; Huang, F.; Zhang, Y.; Cheng, Y.F. Effect of cathodic protection potential fluctuations on pitting corrosion of X100 pipeline steel in acidic soil environment. *Corros. Sci.* **2018**, *143*, 428–437. [CrossRef]
62. Ma, H.; Zhao, B.; Liu, Z.; Du, C.; Shou, B. Local chemistry–electrochemistry and stress corrosion susceptibility of X80 steel below disbonded coating in acidic soil environment under cathodic protection. *Constr. Build. Mater.* **2020**, *243*, 118203. [CrossRef]
63. Wang, X.; Wang, C.; Tang, X.; Guo, Z. Study on Cathodic Protection Parameters of X100 Steel in Three Types of Simulated Soil Solutions. *Int. J. Electrochem. Sci.* **2014**, *9*, 7660–7671. [CrossRef]
64. Ashari, R.; Eslami, A.; Shamanian, M.; Asghari, S. Effect of weld heat input on corrosion of dissimilar welded pipeline steels under simulated coating disbondment protected by cathodic protection. *J. Mater. Res. Technol.* **2020**, *9*, 2136–2145. [CrossRef]
65. Chen, P.; Li, R.; Jia, G.; Lan, H.; Fu, K.; Liu, X. A Decade Review of the Art of Inspection and Monitoring Technologies for Long-Distance Oil and Gas Pipelines in Permafrost Areas. *Energies* **2023**, *16*, 1751. [CrossRef]
66. Ma, Y.B.; Tan, D.J.; Jing, H.Y.; Xue, Q.; Zhang, C.Z. Permafrost Hazard of MoHe-DaQing Crude Oil Pipeline. *Adv. Mater. Res.* **2013**, *734–737*, 2659–2663. [CrossRef]
67. Jamali, S.; Alamuti, M.M.; Savaghebi, M. Effects of different earthing schemes on the stray current in rail transit systems. In Proceedings of the 2008 43rd International Universities Power Engineering Conference, Padova, Italy, 1–4 September 2008; pp. 1–5. [CrossRef]
68. Lee, C.H.; Lu, C.J. Assessment of Grounding Schemes on Rail Potential and Stray Currents in a DC Transit System. *IEEE Trans. Power Deliv.* **2006**, *21*, 1941–1947. [CrossRef]
69. Zhang, B.; Li, L.; Zhang, Y.; Wang, J. Study on the Interference Law of AC Transmission Lines on the Cathodic Protection Potential of Long-Distance Transmission Pipelines. *Magnetochemistry* **2023**, *9*, 75. [CrossRef]
70. Peng, X.; Huang, Z.; Chen, B.; Liu, D.; Li, H. On the interference mechanism of stray current generated by DC tram on pipeline corrosion. *Eng. Fail. Anal.* **2020**, *116*, 104760. [CrossRef]
71. Wang, C.; Wang, Y.; Xu, S.; Li, W.; Wang, Y.; Xing, F. Assessment of interference scope induced by stray current in the metro depot for the corrosion risk of buried metal pipeline. *Electr. Eng.* **2024**, *106*, 4277–4296. [CrossRef]
72. Ding, J.; Liu, X.; Ma, G.; Guo, Y.; Li, X. Corrosion Behavior of Pipelines Influenced by Dynamic Stray Currents Derived from Underground Rail Infrastructure. *ACS Omega* **2026**, *11*, 7475–7485. [CrossRef] [PubMed]
73. Chen, X.; Li, L. Study on the Interference of the HVDC Transmission Grounding Electrode to the Pipeline Cathodic Protection System. *ACS Omega* **2023**, *8*, 22088–22098. [CrossRef] [PubMed]
74. Bertolini, L.; Carsana, M.; Pedeferri, P. Corrosion behaviour of steel in concrete in the presence of stray current. *Corros. Sci.* **2007**, *49*, 1056–1068. [CrossRef]
75. Qin, H.; Du, Y.; Lu, M.; Meng, Q. Effect of dynamic DC stray current on corrosion behavior of X70 steel. *Mater. Corros.* **2020**, *71*, 35–53. [CrossRef]
76. Ormellese, M.; Beretta, S.; Brugnetti, F.; Brenna, A. Effects of non-stationary stray current on carbon steel buried pipelines under cathodic protection. *Constr. Build. Mater.* **2021**, *281*, 122645. [CrossRef]
77. Cui, G.; Li, Z.L.; Yang, C.; Wang, M. The influence of DC stray current on pipeline corrosion. *Pet. Sci.* **2016**, *13*, 135–145. [CrossRef]
78. Xu, J.; Bai, Y.; Wu, T.; Yan, M.; Yu, C.; Sun, C. Effect of elastic stress and alternating current on corrosion of X80 pipeline steel in simulated soil solution. *Eng. Fail. Anal.* **2019**, *100*, 192–205. [CrossRef]
79. Zhu, M.; Du, C.; Li, X.; Liu, Z.; Wang, S.; Li, J.; Zhang, D. Effect of AC current density on stress corrosion cracking behavior of X80 pipeline steel in high pH carbonate/bicarbonate solution. *Electrochim. Acta* **2014**, *117*, 351–359. [CrossRef]
80. Zhu, M.; Du, C.W.; Li, X.G.; Liu, Z.Y. Stress Corrosion Cracking of X80 Pipeline Steel Under Various Alternating Current Frequencies in High-pH Carbonate/Bicarbonate Solution. *CORROSION* **2014**, *70*, 1181–1188. [CrossRef]
81. Liu, Q.; Wu, W.; Pan, Y.; Liu, Z.Y.; Zhou, X.C.; Li, X.G. Electrochemical mechanism of stress corrosion cracking of API X70 pipeline steel under different AC frequencies. *Constr. Build. Mater.* **2018**, *171*, 622–633. [CrossRef]

82. Niazi, H.; Eadie, R.; Chen, W.; Zhang, H. High pH stress corrosion cracking initiation and crack evolution in buried steel pipelines: A review. *Eng. Fail. Anal.* **2021**, *120*, 105013. [CrossRef]
83. Liang, Y.; Du, Y.; Tang, D.; Chen, L.; Zhang, L.; Qiao, L. Research on AC corrosion behavior and corrosion product film evolution of X70 steel under the combined action of AC interference and CP. *Corros. Sci.* **2022**, *197*, 110085. [CrossRef]
84. Chen, L.; Du, Y.; Wang, M.; Liu, Y.; Liang, Y.; Zhu, Z.; Zhang, L. In situ and ex situ investigation on the product films evolution of pipeline steel under AC interference and high cathodic protection conditions. *J. Electroanal. Chem.* **2024**, *967*, 118308. [CrossRef]
85. *ISO 18086:2019*; Corrosion of Metals and Alloys—Determination of AC Corrosion—Protection Criteria. International Organization for Standardization (ISO): Geneva, Switzerland, 2019. Available online: https://www.iso.org/standard/78148.html (accessed on 30 July 2026).
86. Paterlini, L.; Marinelli, A.; Brenna, A.; Ormellese, M. Protection Criteria of Cathodically Protected Pipelines Under AC Interference. *Corros. Mater. Degrad.* **2025**, *6*, 7. [CrossRef]
87. Brenna, A.; Beretta, S.; Ormellese, M. AC Corrosion of Carbon Steel under Cathodic Protection Condition: Assessment, Criteria and Mechanism. A Review. *Materials* **2020**, *13*, 2158. [CrossRef] [PubMed]
88. Brenna, A.; Beretta, S.; Uglietti, R.; Lazzari, L.; Pedeferri, M.; Ormellese, M. Cathodic protection monitoring of buried carbon steel pipeline: Measurement and interpretation of instant-off potential. *Corros. Eng. Sci. Technol.* **2017**, *52*, 253–260. [CrossRef]
89. Mahlobo, M.G.R.; Seadira, T.W.P.; Mabuza, M.M.; Olubambi, P.A. Electrochemical Monitoring of Steel Corrosion in NS4 Solution Under Cathodic Protection Environment: Insights of Electrochemical Impedance Spectroscopy. *Mater. Corros.* **2026**, *77*, 1159–1166. [CrossRef]
90. Adzman, M.R.; Sallehuddin, A.A.M.; Shamsudin, S.R.; Husin, N.M.; Haniff, N.S.M.; Gunasilan, M.; Idris, M.H.; Amirruddin, M. Improved impressed current cathodic protection systems by incorporating a pulse-feeding technique integrated with internet of things capabilities. *Int. J. Electr. Comput. Eng. (IJECE)* **2024**, *14*, 7254. [CrossRef]
91. Gao, B.Y.; Li, Z.H.; Huan, T. Research and Application of Digital Monitoring System for Pulse Current Cathodic Protection of Oil Pipeline. *J. Phys. Conf. Ser.* **2023**, *2594*, 012063. [CrossRef]

Disclaimer/Publisher's Note: The statements, opinions and data contained in all publications are solely those of the individual author(s) and contributor(s) and not of MDPI and/or the editor(s). MDPI and/or the editor(s) disclaim responsibility for any injury to people or property resulting from any ideas, methods, instructions or products referred to in the content.